Theoretical study of the interaction between a magnetic nanotip and a magnetic surface

H. Ness* and F. Gautier
Institut de Physique et de Chimie des Matériaux de Strasbourg, Groupe d'Etude des Matériaux Métalliques, Bâtiment 69, 23 rue du Loess, 67037 Strasbourg Cedex, France
(Received 14 April 1995)

A theoretical study of the electronic structure of transition-metals' magnetic nanotips and of the interaction of such tips with magnetic surfaces is performed within the tight-binding scheme. The real-space recursion method is used to calculate the local densities of states of the interacting tips and surfaces. We consider more especially Fe supported tips and both Cr and Ni magnetic surfaces. A strong enhancement of the magnetic moments is observed on the tip's surfaces and tip's apex atoms. The interaction of such tips with Cr(001) and Ni(001) surfaces is studied in regime for which the adhesive forces are dominant. Different magnetic tip-sample (TS) configurations are considered. The electronic structure of both the tip and sample are found to be substantially modified due to the TS interaction. These modifications lead to the decrease of the corresponding magnetic moments for decreasing TS distances. The TS interaction energy curves, the magnetic TS coupling energy, and the magnetic "exchange" forces are also calculated when the tip's apex is located above high-symmetry surface's sites. Large antiferromagnetic (AP) couplings are found between interacting Fe tip and Cr surface, instead of small ferromagnetic (P) couplings for the Ni surface. According to the values of the magnetic TS "exchange" forces and to their variations upon the considered surface's sites, high spatial resolution is expected for such a magnetic force microscopy. Finally, the experimental feasibility for the measurement of such forces and the influence of the tip's morphology on the magnetic contrast are also examined. To our knowledge, this is the first study of the magnetic coupling energy for tip-sample systems.

I. INTRODUCTION

The atomic force microscopy has proven its ability to study surfaces at the atomic scale.[1] Using nonmagnetic tips, atomic resolution was achieved on different materials (layered materials such as graphite,[2] boron nitride,[3] transition-metal dichalcogenides,[3,4] ionic crystals,[5] and metallic surfaces[6]). On the other hand, by using magnetic tips we can also expect to investigate the surface magnetism with a high spatial resolution and up to the atomic scale. Such a possibility is very interesting for the study of the magnetism of surfaces, clusters, and of surface defects such as steps, magnetic impurities, etc.

Up to now, the magnetic forces measured in the magnetic force microscopy[7] were mostly the long-range magnetic dipolar forces arising from the long-ranged interactions between the magnetic dipole of the tip and of the sample, the magnetic tip being essentially sensitive to the stray fields of the surface. The typical tip-sample (TS) separations are of the order of 10 nm for such long-range force measurements. This allows us to study large-scale features such as magnetic domains, the lateral resolution being of the order of several hundred Å (see Ref. 8 and references therein).

Recent scanning tunneling microscopy experiments using magnetic tips were also performed to study, for example, Cr(001) surfaces.[9] They have shown the importance of the relative orientation of the tip and surface magnetization vectors on the tunneling current, this current being enhanced (reduced) in the case of parallel (antiparallel) orientation of the tip and surface magnetizations. The importance of such different magnetic couplings was first recognized in the conductance model of Slonczewski for two ferromagnets separated by a tunneling barrier.[10] It has been suggested[9,10] that the magnetic forces between the tip and the studied sample can be measured for small TS distances ($d \approx 2-5$ Å). For such distances, the magnetic couplings come from the direct interaction between the tip and sample electronic states. They are thought to be sufficiently large to allow the observation at the atomic scale of the surface magnetic moments distribution. However, the use of this imaging procedure is *a priori* limited to intermediate values of the TS distances between two extreme regimes whose salient features are now briefly discussed.

In the first regime, i.e., for very small TS distances, the forces occur from the overlap between the electronic densities. They are strongly repulsive and are easily measured. However, they lead to strong tip and sample deformations which can be irreversible so that the interpretation of the images can be difficult. In the other extreme regime, i.e., for large TS distances, the attractive forces occur from small van der Waals and magnetic dipolar pair interactions. The resulting forces can be measured by dynamical force measurements which are related to the resonance frequency shift of the corresponding oscillatory cantilever.[11] They do not introduce significant deformations but they are sizable because they result from the superposition of a huge number of individual pair interactions arising from the tip's extremity. Global instabilities can occur when the force gradient exceeds the cantilever spring constant.[12]

In the intermediate regime the tip and sample deformations are assumed to be relatively small. The van der Waals forces are not necessarily negligible but the scale of their variations is related to the tip's radius and is much

0163-1829/95/52(10)/7352(11)/$06.00

larger than the atomic scale we are interested in here. Using both scanning tunneling and atomic force microscopies, Dürig, Züger, and Pohl have extensively studied in this regime the adhesion forces at the atomic scale for bimetallic systems.[13] They have shown that the short-range adhesive forces can be measured for tip-sample distances larger than those for which electrical and mechanical contacts successively occur. In this regime, these adhesive forces between the tip apex atoms and the surface dominate the total interaction force gradient as compared to the corresponding contribution of the long-range van der Waals interactions.[14] These authors have estimated the contribution of these later forces over the whole tip and have found they are nearly constant for the considered TS distances. Similar results have been recently obtained from a theoretical study of the atomic force contrast using the molecular mechanics to determine the interaction and the deformations between a silicon tip and a graphite sample.[15]

In this work, we consider only the intermediate interaction regime as studied experimentally by Dürig, Züger, and Pohl. We focus our interest only on the *magnetic interactions* in this regime. These interactions are determined by subtracting the interaction energies for two different TS magnetic configurations at the same TS distance so that the corresponding contribution of the van der Waals interactions is zero. We are only interested in the general trends of such magnetic interactions, their order of magnitude, and their variations from site to site to assess the feasibility of magnetic force microscopy at the atomic scale. This is why we neglect here as a first step the deformations of the tip and the sample which are thought to be sufficiently small to keep unmodified our present conclusions. From these assumptions, we study the behavior of such short-range magnetic forces versus the TS distances and their dependence upon the magnetic nature of the tip and the sample. We also study the importance of the tip's morphology on its magnetic structure and on the TS interaction. Such phenomena have been shown to be important for nonmagnetic interactions.[16,17]

We investigate in this paper both (i) the magnetism of transition-metals' supported nanotips and (ii) the TS magnetic interactions taking account of the electronic structure of the considered systems. Furthermore, the nanotips we consider here are realistic atomically sharp tips, i.e., pyramidal tips built from up to 30 atoms, deposited on the surface of the same metal. Such nanotips have been already obtained experimentally in the case of transition metals.[18] The interaction between the tip and the sample is calculated versus the TS separation and for different tips' positions above the surface. A large number of inequivalent atoms are perturbed by such an interaction. Therefore *ab initio* self-consistent band-structure calculations for these systems require too large supercells and are difficult to achieve for reasonable computing times. This is why we choose the tight-binding approach to describe the band structure of the TS systems. Furthermore, we use the real-space recursion method in order to calculate the local densities of states (LDOS). Note that this method has been also used to study, for example, the magnetic couplings in transition-metal superlattices and gives the good trends for the oscillatory behavior of the coupling energies.[19]

The paper is organized as follows. We present the method of calculation we use in order to determine the electronic structure of the TS systems (Sec. II). We briefly recall the results obtained for the electronic structure of supported tips and the magnetism of such tips (Sec. III). Then Sec. IV is devoted to the TS interaction, i.e., to the modifications of both tip apex and sample surface LDOS due to their interaction and to the behavior of the tip and sample magnetic moments for different magnetic configurations. Finally, the magnetic coupling energies and the corresponding magnetic forces are presented. The experimental feasibility for measuring such forces is also discussed.

II. METHOD OF CALCULATION

As mentioned above, we use in this study the tight-binding approximation and the real-space recursion method to determine the electronic structure of the systems. The total energy results from two contributions: (i) the attractive band term $E_{\rm bs}$ obtained from the LDOS which are spin dependent for magnetic elements and (ii) the repulsive term E_r ensuring the crystal stability. We restricted our attention to "d" bands, the band energy $E_{\rm bs}$ thus being the electronic contribution due to these "d" electrons. This assumption is sufficient to get a realistic description of the transition-metal's bulk and surface magnetism.[20] Let us now briefly describe the main assumptions used for the calculations.

The spin-dependent tight-binding Hamiltonian H is obtained from the energy levels $\varepsilon_{i\lambda}^{\sigma}=\langle i\lambda\sigma|H|i\lambda\sigma\rangle$ which are spin dependent [$\sigma=(+)$ or $(-)$ is the spin component along the local quantization axis] and from the hopping integrals $t_{\lambda\mu}(\mathbf{R}_{ij})=\langle i\lambda\sigma|H|j\mu\sigma\rangle$ between two orbitals λ and μ located on two different sites i and j connected by the $\mathbf{R}_{ij}$ vector. The hopping integrals are assumed to be spin independent and are obtained from the three Slater-Koster parameters $dd\sigma$, $dd\pi$, and $dd\delta$.[21] These parameters are fitted to recover the bulk band width W_b of the considered elements. For example, the W_b values we have chosen for Cr, Fe, and Ni are $W_b=7.28$, 5.34, and 3.80 eV, respectively.

Furthermore, the hopping integrals $t_{AB}(\mathbf{R})$ between atoms A and B of different chemical species are obtained by the Shiba prescription ($t_{AB}^2=t_{AA}t_{BB}$).[22] They are also assumed to decay continuously with interatomic distances R_{ij} with a hyperbolic cosine analytical form and have zero values when $R_{ij}\geq R_4$ (R_n being the equilibrium distance between two nth nearest neighbors). It has been shown that this peculiar distance dependence of the hopping integrals does not strongly modify the LDOS in comparison to a "classical" exponential dependence.[17]

Within the molecular-field approximation, the exchange splitting Δ_i between the energy levels of spin $(+)$ and $(-)$, i.e., $\Delta_i=\varepsilon_i^{(-)}-\varepsilon_i^{(+)}$ (dropping the orbital symmetry indices), is assumed to be proportional to the local magnetic moment m_i via an effective "exchange integral"

I_i ($\Delta_i = I_i m_i$). The local magnetic moment is defined by $m_i = N_i^{(+)} - N_i^{(-)}$, where N_i^σ is the spin-dependent band filling. We obtain N_i^σ from the-spin dependent LDOS $n_{i\lambda}^\sigma(\varepsilon)$: $N_i^\sigma = \Sigma_\lambda \int^{\varepsilon_F} n_{i\lambda}^\sigma(\varepsilon) d\varepsilon$ (ε_F being the Fermi level).

The exchange splitting and the local magnetic moments are determined in a consistent way, the ratio $(\varepsilon_i^{(-)} - \varepsilon_i^{(+)})/(N_i^{(+)} - N_i^{(-)}) = I_i$ being assumed to depend only on the chemical nature of the considered site i. The values of the exchange integrals are chosen to recover the values of the bulk magnetic moment m_{bulk}. For example, the value of m_{bulk} for Cr, Fe, and Ni are $m_{\text{bulk}} = 0.6$, 2.2, and $0.6\mu_B$, respectively. Furthermore, we required the self-consistent local neutrality on each atomic site. This approximation is valid because the electronegativity difference between the constituents we consider here is not too large. The self-consistency is performed assuming that the energy levels are independent of the considered d orbital symmetry ($\varepsilon_{i\lambda}^\sigma = \varepsilon_i^\sigma$). These levels are determined to obtain the band filling $N_i = N_i^{(+)} + N_i^{(-)}$ within the local neutrality with an accuracy of 10^{-4}. The N_i values we have chosen for Cr, Fe, and Ni are $N_i = 5.0$, 7.0, and 9.4, respectively. In practice, the self-consistent procedure is performed for a limited number of atoms defining the "perturbation domain." This domain is made of the tip's atoms and of those atoms of the tip's support and of the sample's surface which are strongly perturbed by the presence of the tip. This has been already described elsewhere[17] (see, for example, Fig. 1, which represents a schematic top view of the supported tip).

Finally in this model, the band energy E_{bs} is written as the sum of local band energies over all the sites i of the system. These local energies results from the integration of the spin-dependent LDOS $[\Sigma_{\lambda,\sigma} \int^{\varepsilon_F} \varepsilon n_{i\lambda}^\sigma(\varepsilon) d\varepsilon]$, subtracting the electrostatic $[N_i(\varepsilon_i^{(+)} + \varepsilon_i^{(-)})/2]$ and magnetic $[-I_i m_i^2/4]$ local energies which are counted twice in the one-electron LDOS integrals. The repulsive energy E_r is described by a pair potential of the Born-Mayer type, whose parameters are fitted to get the equilibrium lattice parameter, the bulk isotropic compressibility, and cohesive energy.[23]

The spin-dependent LDOS are obtained from the Green's function using the recursion method.[24] The Green's function is expressed as a continued fraction of N exact levels (we have used $N = 8$ recursion levels for the Fe-Cr system and $N = 14$ for the Fe-Ni system[17]) involving the recursion coefficients and terminated in the usual square-root way, the last coefficients being obtained by being obtained by the Beer-Pettifor method.[25]

In this first study, we consider three materials having different magnetic behaviors; i.e., a strong ferromagnet (Ni), a weak ferromagnet (Fe), and an antiferromagnetic material (Cr). Furthermore, we consider only the sharpest possible perfect Fe pyramids (pyr) built from $h = 4$ perfect bcc Fe(001) planes [denoted pyr(001) hereafter]. These tips, having a monoatomic apex, are deposited on the (001) surface of a perfect semi-infinite bcc Fe crystal. The samples are also assumed to be perfect semi-infinite bcc Cr or fcc Ni crystals and are limited by a perfect

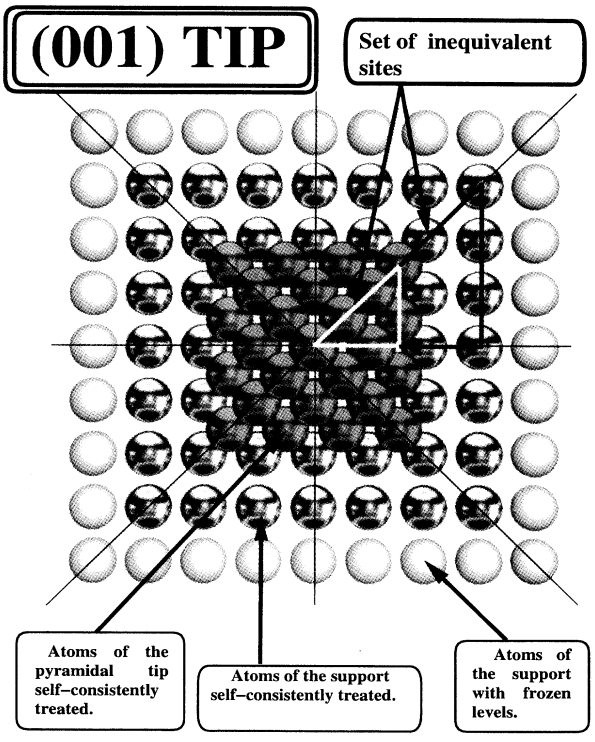

FIG. 1. Schematic top view of the supported pyr(001) $h = 4$ tip. The perturbation domain is defined by the tip and tip's support atoms which are labeled to be "self-consistently" treated. It extends on the first four tip support (001) planes. Note that only a limited extent of the tip's support surface plane is shown. Owing to symmetry properties, the equivalent tip and tip support atoms are contained in the irreducible eighth (white and black triangles, respectively). For simplicity, the perturbation domain on the sample surface is not shown. However, it has the same lateral extent as the ones of the tip's support.

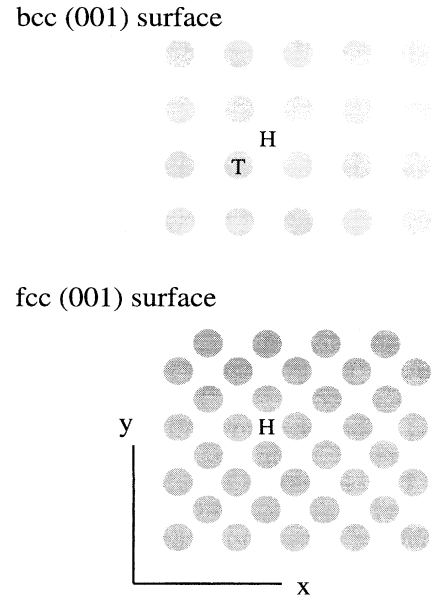

FIG. 2. Schematic representation of the different high symmetry surface sites [hollow (H) and top (T) sites] for both the Cr(001) and Ni(001) surfaces.

(001) surface. The high-symmetry surface sites above which the tip is located are shown in Fig. 2.

Finally, as mentioned in the introduction we assumed that (i) the distance d between the apex and the sample's surface varies only between one and three bulk interplanar distances $d_{(001)}$, i.e., between 1.5 and 4.5 Å; (ii) both transition-metal-based tip and sample are separated rigidly from each other without surface relaxation, reconstruction, or deformations. At this stage it is relevant to comment upon this approximation in relation with recent molecular-dynamics studies of deformations and instabilities for nonmagnetic tip-sample junctions. The instabilities for which both "surfaces" snap together have been studied using semiempirical potentials.[26,27,28] They are strongly dependent upon the tip's morphology and the mechanical properties of the considered systems. For example, the behavior of the hard transition-metal systems—such as Ir—is very different from the one of soft materials such as lead.[27] This has been confirmed by a tight-binding molecular-dynamics study of a Re nanotip interacting with a Re surface.[28] Therefore, the deformations induced by these interactions in the regime we consider here are small for transition metals. Moreover, the magnetic contrast being obtained from a difference of the interaction energies between different TS magnetic configurations, these deformations lead to changes of the contrast which are not relevant as far as general trends for magnetism are concerned.

III. SUPPORTED TIP MAGNETISM

Let us briefly recall the main features of the apex LDOS and describe the results concerning the surface and tip apex magnetism. The apex LDOS width is essentially determined by the number n_i of first and second nearest-neighbor ($i=1,2$, respectively) of the apex atom: $n_1=4$ and $n_2=1$ for pyr(001). It is independent of h and is smaller than or equal to the width of the corresponding surface ($n_1,n_2=4,5$ for (001); 4,3 for (111) surface). No strong surface peak appears near the middle of the apex LDOS as can be seen in Fig. 3.

The surface magnetism and the corresponding magnetic moment enhancement can be qualitatively explained in terms of reduced bandwidths. Within the tight-binding scheme, the reduced bandwidth is related to the reduced number of nearest neighbors for surface or tip apex atoms as compared to bulk atoms. In agreement with such a qualitative criterion, we find large magnetic moments on surfaces and very large magnetic moments on the tip's apex atom. In order to make precise the magnetic moment enhancement and to relate it to the reduction of the coordination number, we list below the values of the Fe and Cr magnetic moments for decreasing values of the coordination number: bcc bulk Fe $m=2.20\mu_B$, Fe(001) surface $m=2.62\mu_B$, Fe(111) $m=2.75\mu_B$, apex of a Fe pyr(001) $h=4$, $m=2.91\mu_B$. For bcc bulk Cr, $m=0.60\mu_B$, Cr(001) $m=2.29\mu_B$, Cr(111) $m=2.98\mu_B$, apex of a Cr pyr(001) $h=4$, $m=3.38\mu_B$. Note that the value of the magnetic moment for the Fe pyr(001) apex is nearly saturated.

Now let us briefly discuss the distribution of the magnetic moments on the Fe pyr(001) $h=4$ tip and its perturbation's extent on the tip's support. Figure 4 shows the magnetic moment distribution on the Fe tip and on the first layers of the Fe(001) tip support. Note that due to the symmetry properties of the tip, only the irreducible eighth of the perturbation domain needs to be represented. The strongly enhanced magnetic moments are those of the less coordinated atoms, i.e., those sitting on the pyramid's surface and more especially the apex atom. The perturbation induced by the tip on its support extends only on the four first surface layers. Moreover, one can notice that out of the range of the tip's support perturbation domain shown in Fig. 4, the magnetic properties of the free surface (i.e., the surface in the absence of

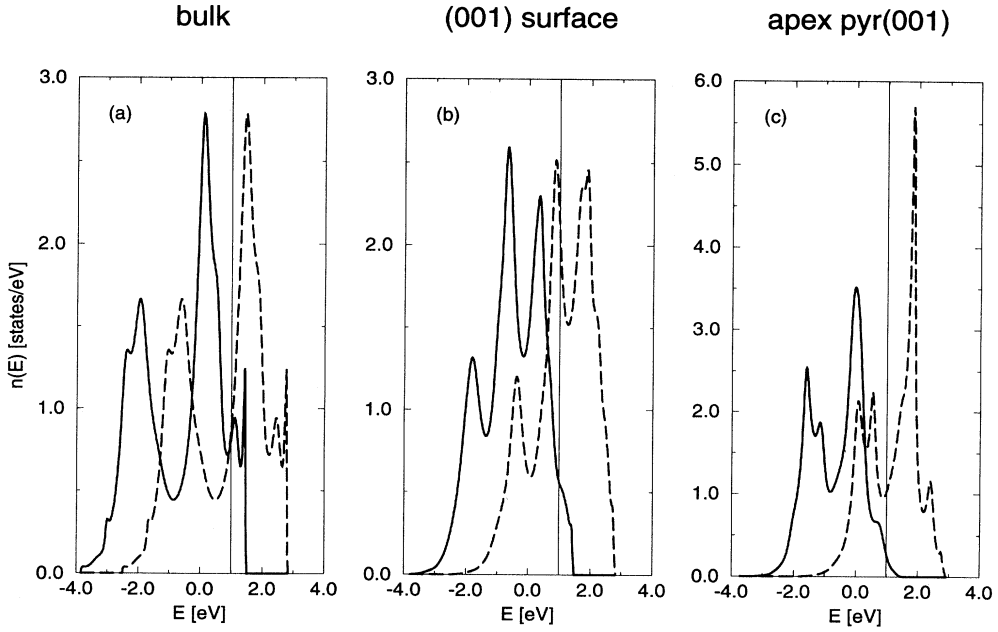

FIG. 3. LDOS of Fe for (a) a bulk atom, (b) a (001) surface atom, and (c) the apex atom of the pyr(001) $h=4$ tip. The energies are given in eV, the values of the density of states are given in states per eV, and the vertical line represents the Fermi level ε_F as in the following LDOS figures.

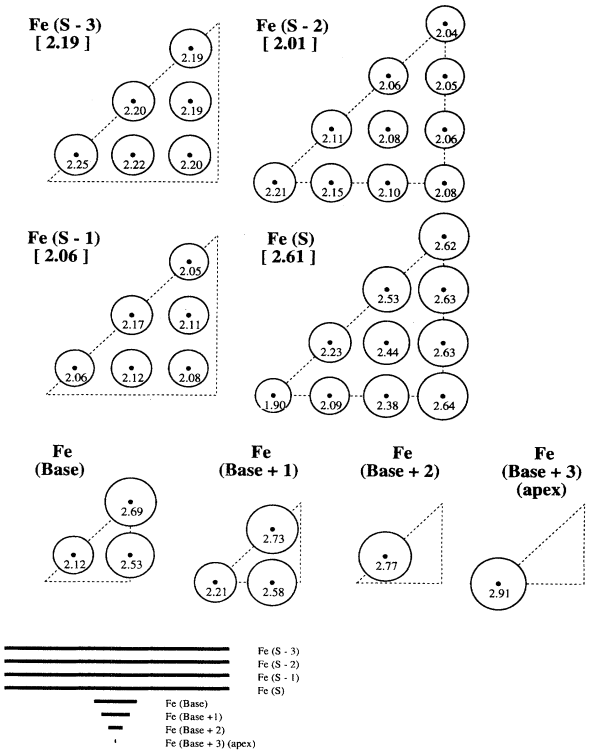

FIG. 4. Magnetic moments distribution on the Fe pyr(001) $h=4$ tip and tip support atoms according to the irreducible eighth defined in Fig. 1. The inset is a simplified representation of the tip and tip support. The values in brackets for the different tip support planes are the values of the magnetic moment for the corresponding planes of a free surface (surface in the absence of the tip). The magnetic moments are given in μ_B.

the tip) are recovered. This clearly shows the localization of the tip's perturbation on its support.

IV. MAGNETIC TIP-SAMPLE INTERACTIONS

We study the magnetic TS interactions in order to understand the origin of the magnetic contrast in magnetic force microscopy at the atomic scale. In order to determine such magnetic "exchange" forces, two different magnetic configurations are considered. Starting from the uncoupled TS system, the "ferromagnetic" (P) configuration ["antiferromagnetic" (AP) configuration] corresponds (respectively) to a parallel (antiparallel) orientation of the magnetic moment of the tip's atoms and of that of the sample's surface. The electronic structure of the interacting system is calculated for decreasing d values and for the two magnetic configurations considered above.

In this section, we calculate the interactions between the perfect Fe supported tip pyr(001) $h=4$ and both Cr(001) and Ni(001) surfaces. We assume that the tip's apex occupies either a hollow surface site (i.e., a site above the center of a square of first surface nearest neighbors) or a top site (i.e., a site on top of a sample's surface atom) such as depicted in Fig. 2.

The following sections are devoted to a discussion of (i) the modifications of the LDOS of the apex and of its sample's surface nearest neighbors, (ii) the behavior of the magnetic moments of the apex atom and of its surface nearest-neighbor atoms depending on the P and AP magnetic configurations and on the nature of the surface site facing the apex, and finally (iii) the TS coupling energies and the corresponding magnetic exchange forces.

A. Modifications of the local densities of states

First we discuss the qualitative modifications of the apex LDOS and of its surface nearest neighbors. As the TS distance decreases, the coordination number of the apex and of its surface nearest neighbors increases. Such a coordination increase implies a broadening of the corresponding LDOS. This broadening is more important for a hollow site than for a top site because the number of bonds participating in the TS interaction is larger for a hollow than for a top site. Moreover, the LDOS of the apex and its surface nearest neighbors are strongly modified due to the strong TS interaction.

For example, when the Fe tip is facing the hollow site of the Cr(001) surface, states above and below ε_F in the apex LDOS are progressively shifted towards the top and bottom of the band as d decreases [Fig. 5(a)]. These shifts induce a strong hole in the middle of the apex LDOS. Note that the surface peak observed in the majority spin band of the Cr(001) surface atoms (nearest neighbors of the apex atom) disappears progressively [Fig. 5(b)]. Another example, which has been already pointed out in the case of nonmagnetic TS systems,[17] concerns the presence of new strong peaks near the top of the bands when the Fe tip is located above a surface top site (A and B peaks in Fig. 6). These peaks, which exist for both spin-dependent LDOS of the Fe tip's apex and of its Cr surface nearest neighbor, are due to the strong interaction between the apex atom and its on-top surface nearest neighbor. They are at the same energies for each spin direction and correspond to strong d_{z^2} directed bonds.

When the Fe tip is facing the hollow site of the Ni(001) surface, one observes the same qualitative behavior. However, owing to the difference of magnetic behavior and of the surface symmetry properties between the Ni and Cr surfaces, the modifications of the Fe apex LDOS are quite different from those described previously. For example, the peak in the minority spin bands just above ε_F behaves differently compared to the Fe-Cr system. This peak, mainly due to the d_{z^2} and $d_{x^2-y^2}$ orbitals, has an increasing magnitude for decreasing d values in the case of the Fe-Ni system (A peak in Fig. 7). This behavior is opposite to the one observed in the Fe-Cr system. Such a difference comes from the following features: (i) the Ni is a strong ferromagnet—note that even for the smallest TS distances shown in Fig. 7, i.e., for $d/d_{\mathrm{Ni}(001)}=0.90$, the majority spin band is still saturated, (ii) the Ni(001) surface LDOS does not present any surface peak, and finally (iii) the $d_{x^2-y^2}$ tip's apex orbital points directly towards the apex nearest-neighbor atoms of Ni(001) surface as shown in Fig. 2 (compare with the effect of the d_{z^2} orbital when the tip is located on top of a surface atom). Finally, the LDOS modifications of the Ni surface atoms, nearest neighbors of the apex, are less marked than those

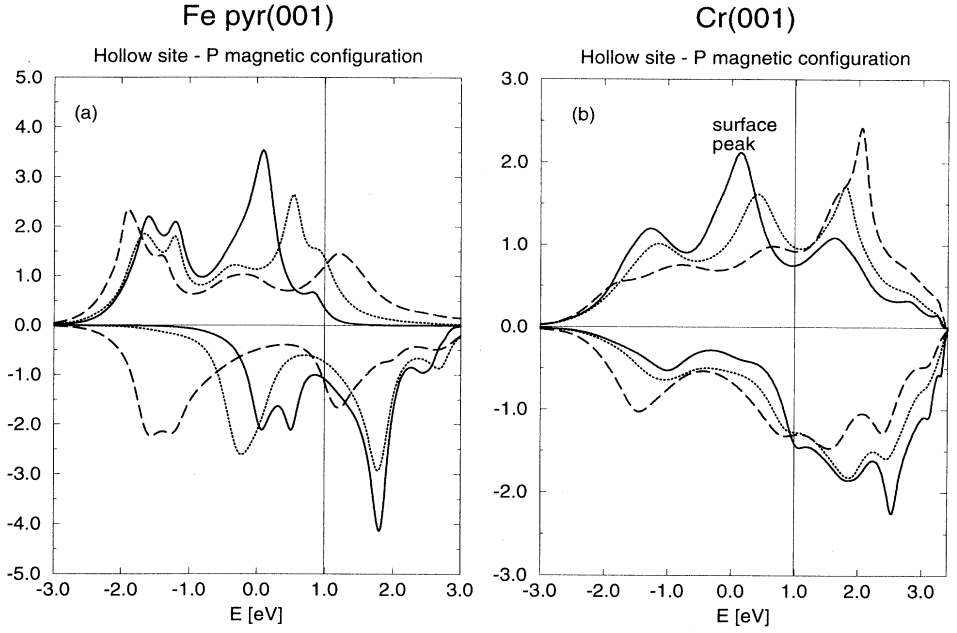

FIG. 5. LDOS of (a) the Fe pyr(001) $h=4$ tip apex and (b) its Cr(001) surface nearest neighbors for different TS distances. The tip is facing a hollow site for the P magnetic configuration. The TS distances are $d/d_{\mathrm{Cr}(001)}=2.00$ (full line), 1.20 (dotted line), and 0.80 (dashed line). The Cr(001) surface peak is also indicated in (b).

of the Cr surface atoms.

This study shows that the TS interaction we consider here involves strong modifications of the LDOS of the apex and of its surface nearest neighbors. However, these modifications depend strongly on the nature of the magnetic behavior of the corresponding chemical species and on the nature of the surface's site facing the tip's apex.

B. Magnetic moments of the apex and of its surface neighbors

From the previous discussions, it is expected that the magnetic moments of the tip's apex atom and of its surface nearest-neighbor atoms decrease when the tip is brought close to the surface. However, the magnetic moment decrease is expected to be different when considering different TS systems and different magnetic configurations.

First let us discuss the results obtained for the Fe-Cr system. The behaviors of the magnetic moments of the apex and its surface nearest neighbors versus the TS distances are shown (for a hollow site) in Fig. 8. The magnetic moments decrease strongly with decreasing d values for both the Fe apex and its Cr surface nearest neighbors. These moments nearly vanish for $d/d_{\mathrm{Cr}(001)} \leq 1.0$ in the case of the P magnetic configuration. The magnetic moments of the surface atoms are always smaller for the P

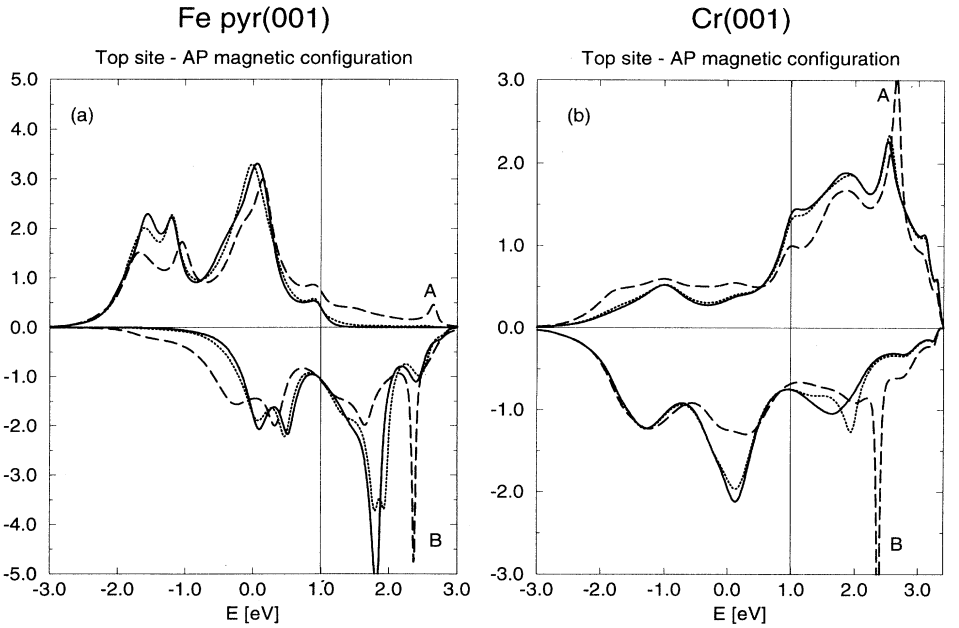

FIG. 6. LDOS of (a) the Fe pyr(001) $h=4$ tip apex and (b) its Cr(001) surface nearest neighbors for different distances d. The tip is facing a top site for the AP magnetic configuration. $d/d_{\mathrm{Cr}(001)}=2.60$ (full line), 2.00 (dotted line), and 1.50 (dashed line). The A and B peaks come mainly for the d_{z^2} orbital.

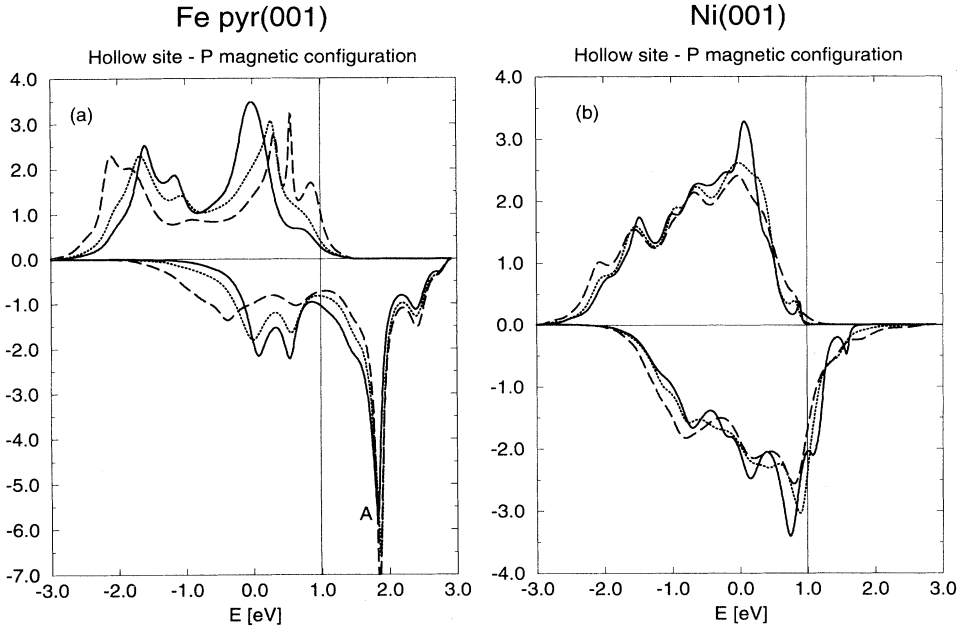

FIG. 7. LDOS of (a) the Fe pyr(001) $h=4$ tip apex and (b) its Ni(001) surface nearest neighbors for different distances d. The tip is facing a hollow site for the P magnetic configuration. $d/d_{\mathrm{Ni}(001)}=2.00$ (full line), 1.20 (dotted line), and 0.90 (dashed line). The A peak comes mainly from the d_{z^2} and $d_{x^2-y^2}$ orbitals.

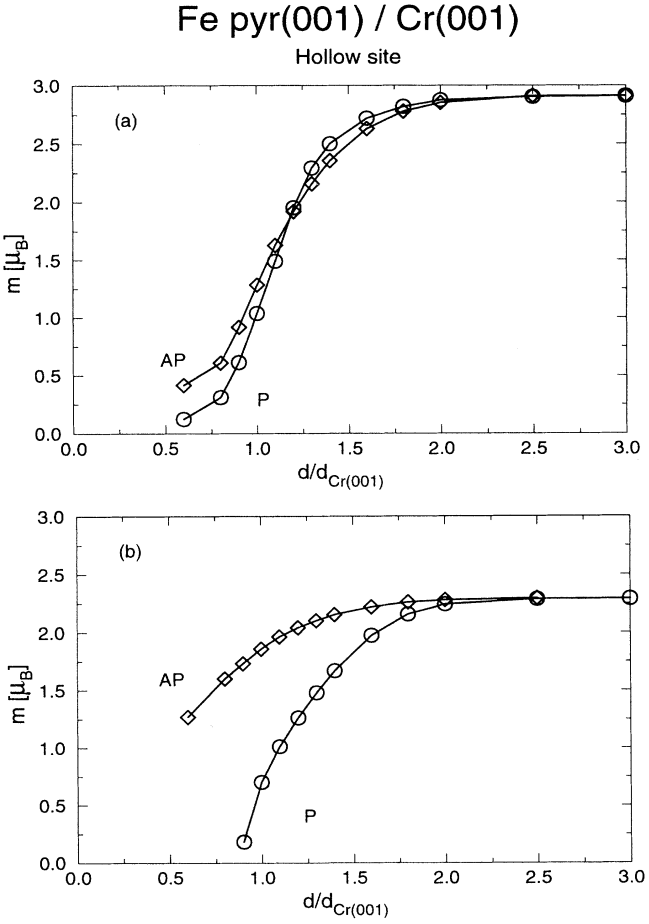

FIG. 8. Magnetic moments of (a) the Fe pyr(001) $h=4$ tip apex and (b) its Cr(001) surface nearest neighbors versus the TS distance for both the P (circles) and AP (squares) magnetic configurations. The tip is facing a hollow site. The magnetic moments of the Cr(001) surface atoms are given in absolute values for the AP configuration (as below).

magnetic configuration than for the AP configuration. However, the apex magnetic moment varies quite differently. Finally, note the strong sensitivity of magnetic moments of the Cr surface atoms to the magnetic configurations as compared to the Fe apex moment.

For the Fe tip facing a top site of the Cr(001) surface, one obtains the same qualitative behavior for the magnetic moments. However, since the TS interaction occurs essentially via the tip's apex and its unique surface nearest neighbor, the decrease of the magnetic moments begins for larger TS distances than in the case of a hollow site as shown, for example, in Fig. 9.

Finally, instabilities of the magnetic moments such as reversal of the moments with respect to the initial magnetic configuration have been observed in the case of the

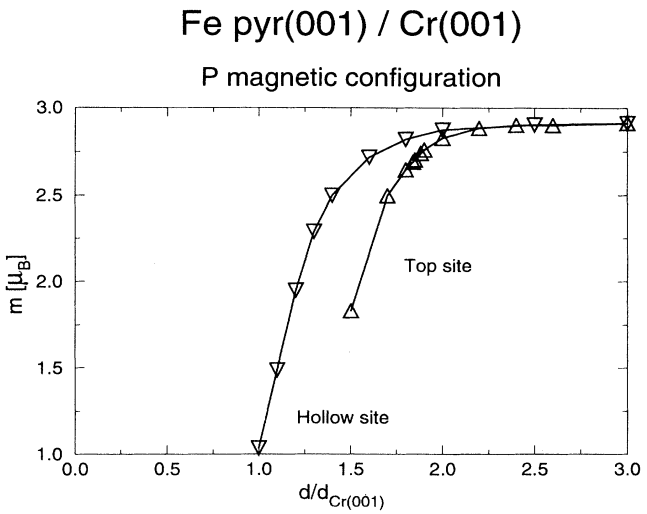

FIG. 9. Magnetic moments of the Fe pyr(001) $h=4$ tip apex interacting with the Cr(001) surface for different tip positions. Only the results for the P magnetic configuration are shown.

P coupling. Note that in these cases the TS separation distances are quite small (slightly smaller than the corresponding interlayer spacing $d_{Cr(001)}$) when the tip is located above a hollow surface site. The TS deformations must be taken into account to confirm such a behavior.

Let us now summarize the results we obtained when considering the two ferromagnetic Fe-Ni systems. We find qualitatively the same behavior for the magnetic moments of the Fe apex and of its Ni surface nearest neighbors for decreasing TS distances (Fig. 10). The main differences between this system and the Fe-Cr system can be summarized as follows: (i) for approximately the same range of TS distances, the decrease of the magnetic moments is much less important for the Ni(001) surface than for the Cr(001); (ii) the magnetic moments decrease faster for the AP magnetic configuration, so that this magnetic configuration is less stable than the P configuration; and (iii) the same relative sensitivity to the P or AP magnetic configuration is observed for both the Fe tip's apex and its Ni surface nearest neighbors, the Fe apex being less sensitive to the difference of magnetic configuration than when such tip interacts with the Cr(001) surface.

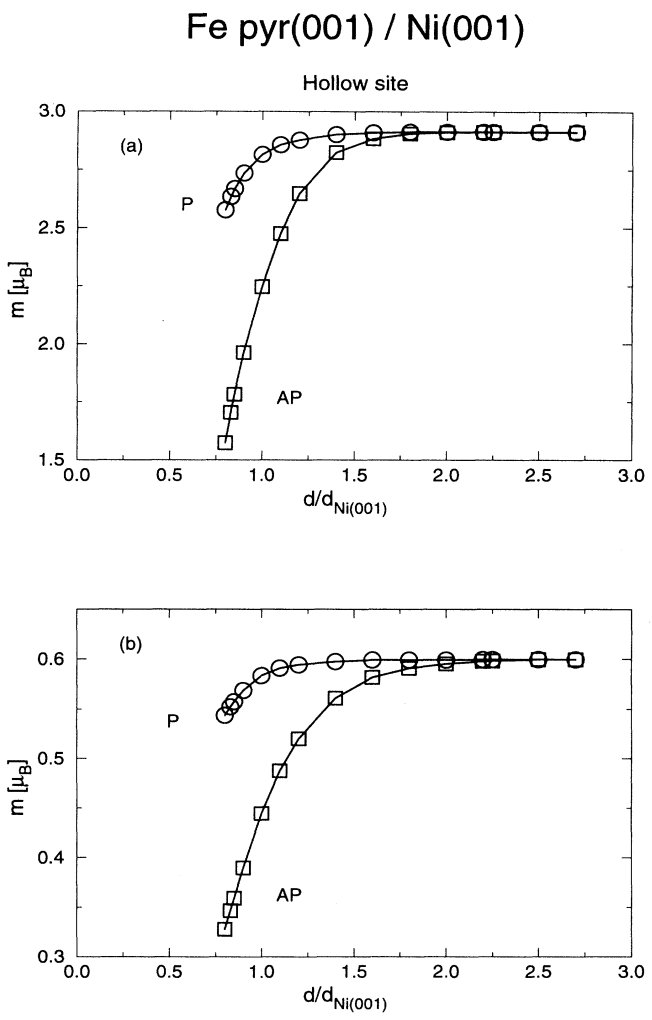

FIG. 10. Magnetic moments of (a) the Fe pyr(001) $h=4$ tip apex and (b) its Ni(001) surface nearest neighbors versus the TS distance for both the P (circles) and AP (squares) magnetic configurations. The tip is facing a hollow site.

In conclusion, this study has emphasized two important features as far as the tip's apex and its surface nearest neighbors are concerned. The magnetic moments are strongly dependent (i) on the nature of the surface site facing the tip's apex and (ii) on the TS magnetic configuration with respect to the magnetic nature of the considered metals (antiferromagnet, strong or weak ferromagnet).

C. Magnetic coupling energies

The TS magnetic coupling energy is defined by the difference of the TS interaction energy between the two magnetic configurations: $E_{\text{coupling}}=E_{\text{int}}(\text{P})-E_{\text{int}}(\text{AP})$. It has been calculated versus the TS distance for the systems considered previously and for different tip positions over the sample's surface.

The results we obtain for the coupling energies are summarized in Fig. 11. According to the previous discussions concerning the behavior of the magnetic moments of the strongly interacting TS atoms, we obtain large AP couplings between the Fe tip and Cr(001) surface and small P couplings for the Ni(001) surface. The values of the couplings' energy extreme E^* and the corresponding TS distances d^* are strongly dependent on the considered surface site. For example, in the case of the Cr(001) surface, the E^* (d^*) values are (respectively) much larger (smaller) for the hollow (top) surface site, the tip and sample interacting via a larger (smaller) number of TS bonds. However, the sign of the couplings (P or AP) is only sensitive to the nature of the tip and sample chemical species.

In order to compare the values of the TS separations corresponding to the coupling energy maxima for the different systems, we have reported the normalized coupling energies in the same figure (Fig. 12), the normalization being done with respect to the E^* values for each system.

Up to now we have only considered atomically sharp

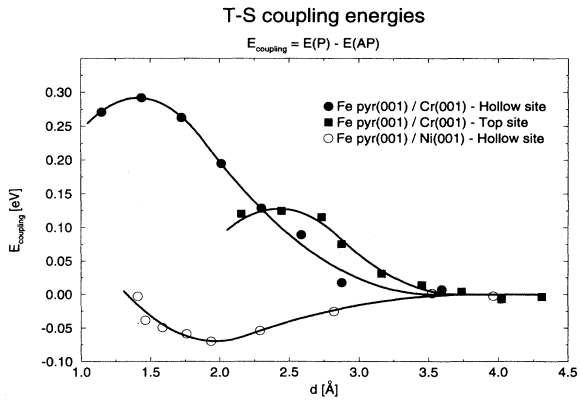

FIG. 11. Coupling energy curves versus the TS distance for both of the different considered systems and surface sites. The TS distances are given in Å.

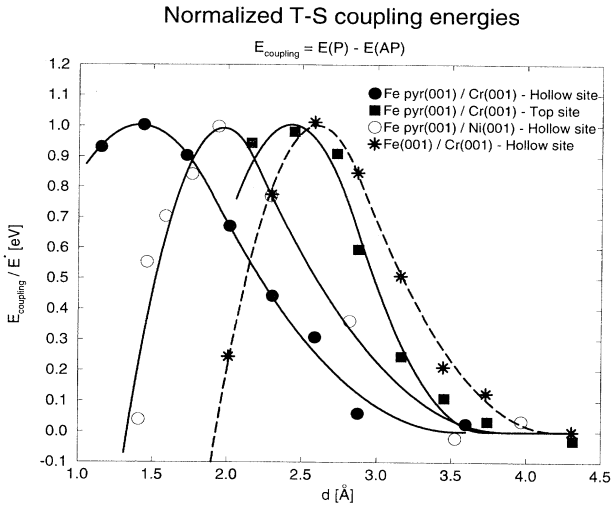

FIG. 12. Normalized coupling energy curves versus the TS distance. The normalization is done with respect to the E^* extrema of the coupling energies given in Fig. 11 for each system. The results obtained for the blunt Fe tip [i.e., a Fe(001) surface] interacting with the Cr(001) surface are also shown (dashed line).

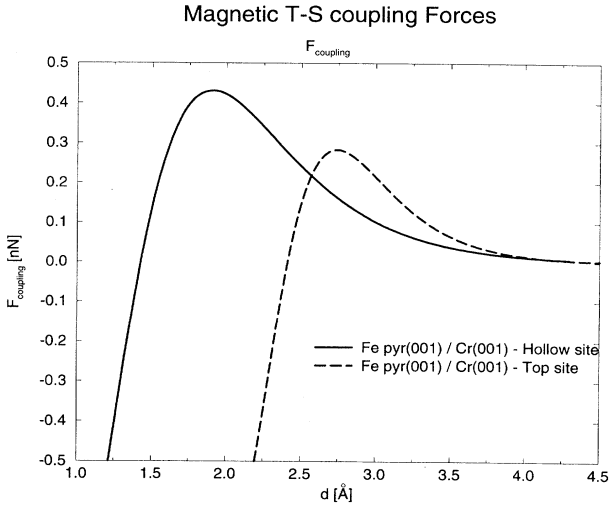

FIG. 13. Magnetic coupling forces versus the TS distance for the Fe pyr(001) $h=4$ tip/Cr(001) surface system. The force curves for both hollow and top sites are shown. The curves are obtained from the opposite of the derivative of the fitting curves reported in Fig. 11.

tips. It is also interesting to study the influence of the tip's morphology on the coupling energies. Hence, we also have considered the other limiting case of a blunt tip. Such a tip is modeled by a semi-infinite Fe(001) surface which is built in registry with the Cr(001) surface. Its apex atoms are then facing hollow sites of the Cr(001) surfaces. The coupling energy values versus the TS distance for such a case are also reported in Fig. 12. The corresponding coupling energy maximum occurs for a TS distance which is larger ($d^* \approx 2.60$ Å) than for the atomically sharp tip ($d^* \approx 1.41$ Å). Note also that the coupling energy maximum E^* obtained for the blunt tip ($E^* \approx 0.03$ eV/at.) is nearly equal to its value for the sharp tip at the same TS distance.

We assume that an N_a apex atom's blunt tip can be well represented by such a periodic Fe(001) blunt tip and Cr(001) surface system. This approximation is valid when N_a is "large," that is, when the contribution of the border atoms of the finite tip apex to the interaction energy (force) is negligible as compared to the contribution of the N_a apex atoms. The choice of N_a is by definition arbitrary. However, in order to study the qualitative trends of the influence of the tip's morphology, we choose below the value $N_a=40$ for a typical blunt tip.

D. Can magnetic coupling forces be experimentally observed?

Let us now discuss the results obtained for the TS magnetic coupling forces. These magnetic forces are defined by $F_{\text{coupling}} = -\nabla_d E_{\text{coupling}}$. The values of such magnetic forces for a sharp Fe tip interacting with the Cr(001) surface are reported in Fig. 13. The values of the force maxima are 0.43 nN for a hollow surface site, and 0.28 nN for a top site, the corresponding TS distances being, respectively, $d \approx 1.90$ and 2.72 Å. The values of the TS magnetic coupling forces are expected to be accessible to experimental measurements. Furthermore, their variations with respect to the considered surface site could lead to a high spatial resolution for such a magnetic force microscopy.

As mentioned in the introduction, force measurements on metallic surfaces are often performed using the shift of the cantilever's resonance frequency induced by the TS interaction.[13] This frequency shift is related to the corresponding TS force gradients. This is why it is important to report some representative values of the force gradient for the sharp Fe tip-Cr(001) surface system. For example, the values of the force gradient maxima are approximately 4 N/m for the hollow surface site ($d \approx 2.3$ Å) and 3 N/m for the top site ($d \approx 3.0$ Å) Such force gradients can exceed 100 N/m ($d \approx 3.2$ Å) in the case of the blunt Fe tip (with $N_a=40$ apex atoms) considered in the preceding section.

Another possibility to detect the variation of the TS interaction forces versus the magnetic configuration is the observation of the monoatomic step heights. Such experiments have been recently performed on Cr(001) surfaces by constant tunneling current imaging.[9] In this case, the variation of the step height comes from the variation of the conductance of the TS tunneling junction versus the relative orientation of the magnetizations of the tip and the sample, the Cr(001) surface being assumed to present terraces (separated by monoatomic steps) whose magnetizations are opposite from one terrace to the next. For the magnetic force microscope used in the constant interaction force mode, it is also expected to observe such a step height's variation due to the force difference between the P and AP magnetic configurations.

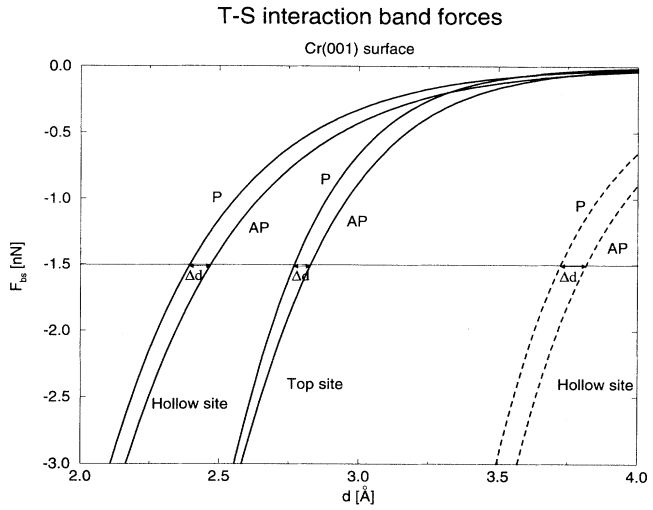

FIG. 14. Band contribution to the TS interaction forces ($F_{bs} = -\nabla_d E_{bs}$) versus the TS distance for both the P and AP magnetic configurations. Different tips facing the Cr(001) surface have been considered: a sharp Fe pyr(001) $h = 4$ tip facing a hollow and a top surface sites (full lines) and a blunt Fe tip (with $N_a = 40$ apex atoms) facing a hollow site (dashed lines). It is shown that the Δd values for a given constant force are not strongly dependent on the tip's morphology.

We have reported in Fig. 14 the values of such TS interaction forces for both the P and AP magnetic configurations in the case of Fe tips interacting with the Cr(001) surface. Only the "band term" force ($F_{bs} = -\nabla_d E_{bs}$) is reported in the figure because, in the present model, this is the only contribution to the total TS interaction force which is dependent on the magnetic configuration. We are only interested in the difference Δd of the TS distances between P and AP magnetic configurations for a given constant force. Δd is related to the large step height values Δh^L and small step height Δh^S by $\Delta d = \frac{1}{2}(\Delta h^L - \Delta h^S)$. For a constant force of $F_{bnd} = -1.50$ nN; the Δd values are approximately 0.07 Å for a hollow surface site and 0.06 Å for a top site. The most striking fact is that such a magnetic contrast does not strongly vary with the tip's morphology. Indeed, for the blunt Fe tip (with $N_a = 40$ apex atoms), the value of the magnetic contrast is only $\Delta d = 0.09$ Å. This implies that for such a measurement of the magnetic contrast, it is not necessary to deal with an atomically sharp tip. However, as mentioned above, the atomically sharp tip is always needed to achieve a lateral high spatial resolution. Finally, if the measurement of such step height is experimentally achievable, Δd will be opposite to the one observed by scanning tunneling microscopy.

V. CONCLUSION

In this paper, we have investigated the interaction of magnetic Fe supported tips with magnetic Cr(001) and Ni(001) surfaces. The band structure of the considered TS systems is described within the tight-binding approximation and the LDOS are determined by the real space recursion method. The electronic and magnetic structure of the interacting tip and sample atoms, the TS interaction energies, are calculated versus the TS distances when the tip is facing high symmetry surface sites. Two magnetic configurations have been considered: the P and AP configurations, for which the tip and sample surface magnetizations are parallel or antiparallel, respectively.

The study of the tip's electronic structure has revealed that the reduced coordination number of the tip's surface and apex atoms leads to an enhancement of the corresponding magnetic moments as compared to the bulk magnetic moments. In the case of an Fe apex atom, the magnetic moment is nearly saturated ($2.91\mu_B$).

We have studied the TS magnetic interaction within the intermediate TS interaction regime (i.e., for $d \approx 2-5$ Å). The LDOS of the apex and of its surface nearest neighbors change drastically for decreasing TS distances. The observation of a strong hole in the middle of the bands or of new peaks occurring from strong directed TS bonds depends on the nature of the surface sites facing the tip's apex. The corresponding magnetic moments' decrease is also sensitive on this parameter. However, the behavior of the magnetic moments and the influence of the magnetic configuration on their values are strongly dependent on the chemical species of the considered atoms. For example, the magnetic moment decrease is less marked for the Ni atoms than for the Cr atoms, the Fe tip apex being an intermediate case. The Cr surface atoms are very sensitive to the magnetic configuration between the tip and the sample. For example, in the case of P configuration, the Fe tip can induce strong perturbations on the Cr(001) surface magnetism.

Finally, considering the TS magnetic coupling energies, we obtain large AP couplings between the Fe tip and the Cr(001) surface and small P couplings for the Ni(001) surface. The corresponding TS magnetic coupling forces are also calculated. The variations of these forces according to the considered surface sites are expected to lead to high spatial resolution for such a magnetic force microscopy. The experimental measurement of the magnetic coupling forces and the influence of the tip's morphology on the magnetic contrast have been also examined.

ACKNOWLEDGMENTS

H.N. would like to thank Dr. U. Dürig and Dr. P. Grütter for fruitful discussions concerning the experimental feasibility for the observation of magnetic "exchange" forces.

*Present address: Department of Physics, University of Durham, Science Laboratories, South Road, Durham DH1 3LE, United Kingdom. Electronic address: Herve.Ness@durham.ac.uk

[1]G. Binnig, C. F. Quate, and Ch. Gerber, Phys. Rev. Lett. **56**, 930 (1986); U. Dürig, J. K. Gimzewski, and D. W. Pohl, *ibid.* **57**, 2403 (1986).

[2]G. Binnig, Ch. Gerber, E. Stoll, T. R. Albrecht, and C. F. Quate, Europhys. Lett. **3**, 1281 (1987); Surf. Sci. **189/190**, 1 (1987); O. Marti, B. Drake, and P. K. Hansma, Appl. Phys. Lett. **51**, 484 (1987); O. Marti, B. Drake, S. Gould, and P. K. Hansma, J. Vac. Sci. Technol. A **6**, 287 (1988).

[3]T. R. Albrecht and C. F. Quate, J. Appl. Phys. **62**, 2599 (1987); J. Vac. Sci. Technol. A **6**, 271 (1988).

[4]E. Meyer, D. Anselmetti, R. Wiesendanger, H. J. Güntherodt, F. Levy, and H. Berger, Europhys. Lett. **9**, 695 (1989).

[5]E. Meyer, H. Heinzelmann, H. Rudin,and H. J. Güntherodt, Z. Phys. B **79**, 3 (1990); G. Meyer and N. M. Amer, Appl. Phys. Lett. **56**, 2100 (1990).

[6]S. Manne, H. J. Butt, S. Gould, and P. K. Hansma, Appl. Phys. Lett **56**, 1758 (1990); S. Manne, P. K. Hansma, J. Massie, V. B. Elings, and A. A. Gewirth, Science **251**, 184 (1991).

[7]Y. Martin and H. K. Wickramasinghe, Appl. Phys. Lett. **50**, 1455 (1987); J. J. Saenz, N. Garcia, P. Grütter, E. Meyer, H. Heinzelmann, R. Wiesendanger, L. Rosenthaler, H. R. Hidber, and H. J. Güntherodt, J. Appl. Phys. **62**, 4293 (1987).

[8]A. Wadas and P. Grütter, Phys. Rev. B **39**, 12 013 (1989); P. Grütter, H. J. Mamin, and D. Rugar, in *Scanning Tunneling Microscopy II,* Vol. 28 of Springer Series in Surface Sciences, edited by R. Wiesendanger and H. J. Güntherodt (Spring-Verlag, Berlin, 1991), p. 151.

[9]R. Wiesendanger, H. J. Güntherodt, R. J. Gambino, and R. Ruf, Phys. Rev. Lett. **65**, 247 (1990); R. Wiesendanger, D. Bürgler, G. Tarrach, A. Wadas, D. Brodbeck, H. J. Güntherodt, G. Güntherodt, R. J. Gambino, and R. Ruf, J. Vac. Sci. Technol. B **9**, 519 (1991).

[10]J. C. Slonczewski, Phys. Rev. B **39**, 6995 (1989).

[11]U. Dürig, O. Züger, and A. Stalder, J. Appl. Phys. **72**, 1778 (1992).

[12]F. O. Goodman and N. Garcia, Phys. Rev. B **43**, 4728 (1991).

[13]U. Dürig, O. Züger, and D. W. Pohl, J. Microsc. **152**, 259 (1988); Phys. Rev. Lett. **65**, 349 (1990).

[14]U. Dürig and O. Züger, in *Nanostructures and Manipulation of Atoms Under High Fields and Temperatures: Applications,* Vol. 235 of NATO ASI, Series E: Applied Sciences, edited by Vu Thien Binh, N. Garcia, and K. Dransfeld (Kluwer Academic, Dordrecht, 1993), p. 271.

[15]H. Tang, C. Joachim, and J. Devillers, Surf. Sci. **291**, 439 (1993); H. Tang, thesis, University Paul Sabatier, Toulouse, France, 1995.

[16]C. Noguera, in *Scanning Tunneling Microscopy III,* Vol. 29 of Springer Series in Surface Sciences, edited by R. Wiesendanger and H. J. Güntherodt (Springer-Verlag, Berlin, 1993), p. 51.

[17]H. Ness and F. Gautier, J. Phys. Condens. Matter **7**, 6625 (1995); **7**, 6641 (1995).

[18]Vu Thien Binh, J. Microsc. **152**, 355 (1988); Surf. Sci. **202**, L539 (1988); Vu Thien Binh and N. Garcia, Ultramicrosc. **42-44**, 80 (1992); Vu Thien Binh and N. Garcia, Surf. Sci. Lett. **320**, L69 (1994).

[19]D. Stoeffler and F. Gautier, J. Magn. Magn. Mater. **121**, 259 (1993), and references therein.

[20]J. Friedel, in *The Physics of Metals,* edited by J. M. Ziman (Cambridge University Press, Cambridge, 1969), p. 494; G. Allan, Surf. Sci. **74**, 79 (1978); Phys. Rev. B **19**, 474 (1979).

[21]J. C. Slater and G. F. Koster, Phys. Rev. **94**, 1498 (1954).

[22]H. Shiba, Prog. Theor. Phys. **46**, 77 (1971).

[23]F. Ducastelle and F. Cyrot-Lackmann, J. Phys. Chem. Solids **31**, 1295 (1970).

[24]R. Haydock, Solid State Phys. **35**, 215 (1980).

[25]N. Beer and D. G. Pettifor, in *The Electronic Structure of Complex Systems,* edited by P. Phariseau and W. M. Temmerman (Plenum, New York, 1984), p. 769.

[26]J. B. Pethica and A. P. Sutton, J. Vac. Sci. Technol. A **6**, 2490 (1988).

[27]A. P. Sutton, J. B. Pethica, H. Rafii-Tabar, and J. A. Nieminen, in *Electron Theory in Alloy Design,* edited by D. G. Pettifor and A. H. Cottrell (The Institute of Materials, London, 1992), p. 191.

[28]U. Landman, W. D Luedtke, N. A. Burnham, and R. J. Colton, Science **248**, 454 (1990).

[29]L. Pizzagalli, S. Bouette, D. Stoeffler, and F. Gautier (unpublished).

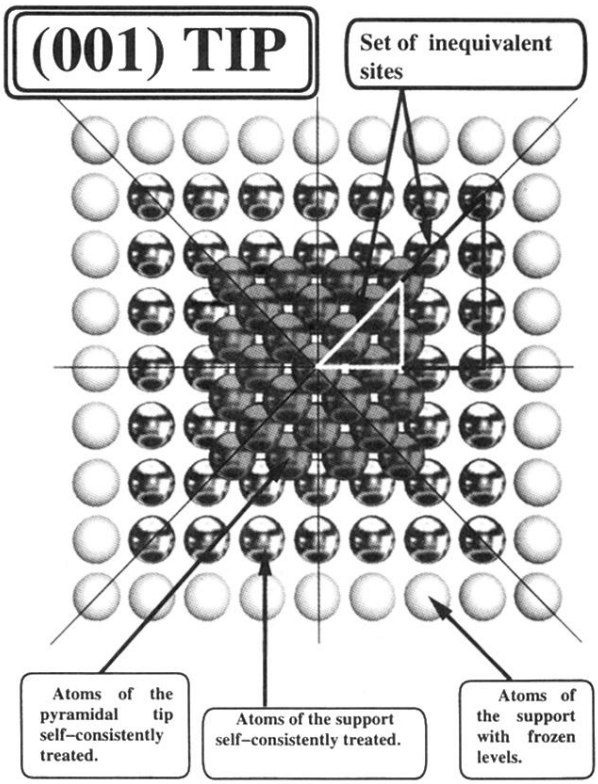

FIG. 1. Schematic top view of the supported pyr(001) $h=4$ tip. The perturbation domain is defined by the tip and tip's support atoms which are labeled to be "self-consistently" treated. It extends on the first four tip support (001) planes. Note that only a limited extent of the tip's support surface plane is shown. Owing to symmetry properties, the equivalent tip and tip support atoms are contained in the irreducible eighth (white and black triangles, respectively). For simplicity, the perturbation domain on the sample surface is not shown. However, it has the same lateral extent as the ones of the tip's support.